References

[1] Schmit, L. A., Morrow, W. M., and Kicher, T. P., "A Structural Synthesis Capability for Integrally Stiffened Cylindrical Shells," AIAA Paper 68-327, Palm Springs, Calif., 1968.

[2] Fox, R. L., and Schmit, L. A., "Advances in the Integrated Approach to Structural Synthesis," *Journal of Spacecraft and Rockets*, Vol. 3, No. 6, June 1966, pp. 858–866.

[3] Fiacco, A. V. and McCormick, G. P., "The Sequential Unconstrained Minimization Technique for Nonlinear Programming, Primal-Dual Method," *Management Science*, Vol. 10, No. 2, Jan. 1964, pp. 360–366.

[4] Fiacco, A. V. and McCormick, G. P., "Computational Algorithm for the Sequential Unconstrained Minimization Technique for Nonlinear Programming," *Management Science*, Vol. 10, No. 4, July 1964, pp. 601–617.

[5] Ralston, A. and Wilf, H. S., *Mathematical Methods for Digital Computers*, Vol. I, Wiley, New York, 1960.

[6] Faddeeva, V. N., *Computational Methods in Linear Algebra*, Dover, New York, 1959, pp. 79–84.

[7] Fox, R. L. and Kapoor, M. P., "Rates of Change of Eigenvalues and Eigenvectors," *AIAA Journal*, Vol. 6, No. 12, 1968, pp. 2426–2429.

[8] Kapoor, M. P., "Automated Optimum Design of Structures under Dynamic Response Restrictions," Rept. 28, 1969, Division of Solid Mechanics, Structures and Mechanical Design, Case Western Reserve University, Cleveland, Ohio.

[9] Davidenko, D. F., "An Approximate Solution of System of Nonlinear Equations," *Ukrain Journal of Mathematics*, Vol. 5, No. 2, 1953, pp. 196–206.

[10] Yakolev, M. N., "The Solutions of Systems of Nonlinear Equations by a Method of Differentiation with Respect to a Parameter," *U.S.S.R. Comput. Math. and Mechanics*, Pt. I, Vol. 4, No. 1, 1964, pp. 198–203.

[11] Kane, T. R., "Real Solutions of Sets of Nonlinear Equations," *AIAA Journal*, Vol. 4, No. 10, 1966, pp. 1880–1881.

[12] Wilde, N. G., "A Note on a Differential Equation Approach to Nonlinear Programming," *Management Science*, Vol. 15, No. 11, 1969, p. 739.

Axisymmetric Ablation with Shape Changes and Internal Heat Conduction

L. A. Popper,* T. Y. Toong,† and G. W. Sutton‡

Avco Everett Research Laboratory, Everett, Mass.

Nomenclature

c_p = specific heat at constant pressure
E = defined in Eq. (19)
F = energy required to ablate unit mass of body
H = total enthalpy
k = thermal conductivity
L = body length (Fig. 1)
p = pressure
q_i = heat flux across inside surface
q_o = heat flux across outside surface
r = radial position (Fig. 1)
R = radial coordinate of the cut-off point (Fig. 1)
R_n = nose radius = $(-r_{st}''')^{-1/2}$
s = recession depth in axial direction
t = time
T = temperature at a position (r, ϕ, t)
T_i = initial temperature of body
u = velocity
x = distance along the curved surface
z = axial position (Fig. 1)
z_i = axial position of original surface at fixed radial position (Fig. 1)
α = thermal diffusivity
β = angle between local surface tangent in meridian plane and axis of symmetry
γ = ratio of specific heats
δ = cone half-angle
μ = viscosity
ξ = defined in Eq. (10)
ρ = material density of the ablating body
ρ_{st} = shocked air density at stagnation point
ϕ = transformed geometric variable (Eq. (1))
ω = temperature exponent for viscosity variation

Subscripts

e = boundary-layer edge condition
n = components normal to local surface
st = stagnation point
∞ = ambient conditions
w = surface
$'$ = d/dx

Presented as Paper 70-199 at the AIAA Aerospace Sciences Meeting, New York, January 19–21, 1970; submitted December 19, 1969; revision received June 25, 1970. This work has been supported by Reentry Physics Division, Army Ballistic Missile Defense Agency, Huntsville, Ala. under Contract DAAH01-68-C-2101. The authors wish to thank John Cronin of AERL who efficiently performed the computer programming and carried out the numerical calculations.

* Senior Engineer. Member AIAA.

† Consultant; also Professor of Mechanical Engineering, Massachusetts Institute of Technology, Cambridge, Mass. Associate Fellow AIAA.

‡ Principal Research Scientist. Fellow AIAA.

I. Introduction

THIS paper presents the effects of internal heat conduction and shape change on the calculation of the ablation of a metal nose tip. This combined problem has not been considered previously. For example, Benjamin[1] introduces the effects of the shape change on the stagnation-point heat flux for sphere-cones in the form of correction factors to the results one would obtain without the effects of geometry change on the heat flux. Transverse heating effects in Ref. 1 are not considered; instead, an effective heat of ablation is introduced. Diffusion of heat in the direction tangential to the surface is also neglected in Ref. 2 compared with that in the direction normal to the surface.

In this paper, a theoretical approach is presented which couples the instantaneous body geometry with the external heating environment and considers the internal flow of heat by thermal heat conduction for blunt-nosed, axially symmetric bodies at hypersonic speeds. Local heat-transfer rates are calculated to correspond to instantaneous boundary-layer growth which varies with flight trajectory and changing body shape. A Landau transformation modified for axisymmetric bodies is used to allow for a receding surface in a three-dimensional coordinate system, such that one of its coordinates remains fixed at the moving surface (Fig. 1).

The general method is applicable whether the ablation is due to melting, sublimation or surface reaction. Results for a

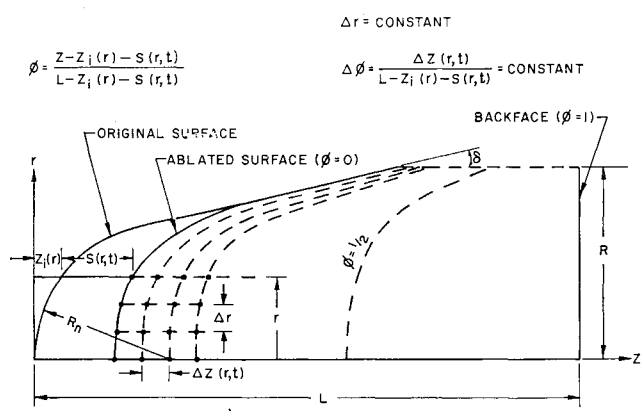

Fig. 1 Schematic diagram of the transformed coordinate system.

beryllium configuration of a typical re-entry vehicle under typical re-entry conditions are presented. The calculation was carried out in the laminar portion of the re-entry; however, it can be extended easily to the turbulent regime by introducing an appropriate criterion for transition and by applying turbulent boundary-layer theory to obtain the aerodynamic heat-transfer rate.

The coupled equations are solved numerically by an explicit technique with the aid of an IBM 360/44 computer. For simplicity, constant material properties were used throughout the calculation.

II. Method of Analysis

a) *Modified Landau transformation*

For thermal-conduction problems involving possible surface recession, it is convenient to use a coordinate system so that one of its coordinates remains fixed at the moving surface. Such a transformation has been used by Landau[3] for a one-dimensional application. This is modified in this study for axisymmetric bodies.

Fig. 1 shows a schematic diagram of the grids in the transformed coordinate system for an axisymmetric body. The spatial coordinates (r,z) are transformed into (r,ϕ) by the use of the following expression

$$\phi(r,z,t) \equiv z - [z_i(r) - s(r,t)]/[L - z_i(r) - s(r,t)] \quad (1)$$

where z_i is the axial position of the original surface at a given radius, s is the change in the axial position from its initial position due to recession, and L is any convenient length chosen to satisfy speicfic boundary conditions. Thus, $\phi = 1$ always corresponds to the back surface.

Using the chain rule of differentiation, one can derive the following:

$$\left(\frac{\partial}{\partial t}\right)_{r,z} = \left(\frac{\partial}{\partial t}\right)_{r,\phi} - \left(\frac{1-\phi}{L - z_i - s}\right)\left(\frac{\partial s}{\partial t}\right)\left(\frac{\partial}{\partial \phi}\right)_{r,t}$$

$$\left(\frac{\partial}{\partial z}\right)_{r,t} = \frac{1}{(L - z_i - s)}\left(\frac{\partial}{\partial \phi}\right)_{r,t}$$

$$\left(\frac{\partial^2}{\partial z^2}\right)_{r,t} = \frac{1}{(L - z_i - s)^2}\left(\frac{\partial^2}{\partial \phi^2}\right)_{r,t}$$

$$\left(\frac{\partial}{\partial r}\right)_{z,t} = \left(\frac{\partial}{\partial r}\right)_{\phi,t} - \left(\frac{(1-\phi)}{(L - z_i - s)}\right) \times \left(\frac{dz_i}{dr} + \frac{\partial s}{\partial r}\right)\left(\frac{\partial}{\partial \phi}\right)_{r,t}$$

$$\left(\frac{\partial^2}{\partial r^2}\right)_{z,t} = \left(\frac{\partial^2}{\partial r^2}\right)_{\phi,t} - \frac{2(1-\phi)}{(L - z_i - s)}\left(\frac{dz_i}{dr} + \frac{\partial s}{\partial r}\right) \times \left(\frac{\partial^2}{(\partial r \partial \phi)}\right)_t + \frac{(1-\phi)^2}{(L - z_i - s)^2}\left(\frac{dz_i}{dr} + \frac{\partial s}{\partial r}\right)^2\left(\frac{\partial^2}{\partial \phi^2}\right)_{r,t} - \frac{(1-\phi)}{(L - z_i - s)}\left\{\frac{d^2 z_i}{dr^2} + \frac{\partial^2 s}{\partial r^2} + \frac{2}{(L - z_i - s)}\left(\frac{dz_i}{dr} + \frac{\partial s}{\partial r}\right)^2\right\}\left(\frac{\partial}{\partial \phi}\right)_{r,t} \quad (2)$$

b) *Transformed thermal-conduction equation*

In cylindrical coordinates, the unsteady thermal-conduction equation for an axisymmetric body with constant thermal conductivity is as follows:

$$\partial T/\partial t = \alpha[\partial^2 T/\partial r^2 + (1/r)\,\partial T/\partial r + \partial^2 T/\partial z^2] \quad (3)$$

where T is the temperature at a position (r,z) and time t, and α is the thermal diffusivity.

By use of Eqs. (2), one obtains the following transformed partial-differential equation in (r,ϕ,t) coordinates:

$$\frac{\partial T}{\partial t} = \frac{\alpha}{(L - z_i - s)^2}\left[1 + (1-\phi)^2\left(\frac{dz_i}{dr} + \frac{\partial s}{\partial r}\right)^2\right] \times \frac{\partial^2 T}{\partial \phi^2} + \alpha\left[\frac{1}{r}\frac{\partial T}{\partial r} + \frac{\partial^2 T}{\partial r^2}\right] - \frac{2\alpha\,(1-\phi)}{(L - z_i - s)} \times \left(\frac{dz_i}{dr} + \frac{\partial s}{\partial r}\right)\frac{\partial^2 T}{\partial r \partial \phi} + \frac{(1-\phi)}{(L - z_i - s)}\left\{\left(\frac{\partial s}{\partial t}\right) - \alpha \times \left[\frac{d^2 z_i}{dr^2} + \frac{\partial^2 s}{\partial r^2} + \frac{2}{(L - z_i - s)}\left(\frac{dz_i}{dr} + \frac{\partial s}{\partial r}\right)^2 + \frac{1}{r}\left(\frac{dz_i}{dr} + \frac{\partial s}{\partial r}\right)\right]\right\}\frac{\partial T}{\partial \phi} \quad (4)$$

c) *Initial and boundary conditions*

i) Initial conditions

$$T(r,\phi,0) = T_i \quad (5)$$

where T_i is the initial temperature of the body, assumed uniform throughout.

ii) Boundary conditions; the heat balance for an infinitesimal control volume across the instantaneous ablating surface requires that

$$q_{i,n} = q_{0,n} - \rho F(\partial s/\partial t)\sin\beta \quad (6)$$

where $q_{i,n}$ and $q_{0,n}$ are the components of q_i and q_0, respectively, normal to the local surface, ρ is the material density of the ablating body, F is the energy required to ablate unit mass of the body, and β is the angle made by the local tangent in a meridian plane from the z axis, such that $\cot\beta = (dz_i/dr + \partial s/\partial r)$. $\rho(\partial s/\partial t)\sin\beta$ represents the mass fluxes across the surface.

In (r,ϕ,t) coordinates, by the use of Eqs. (2) and (6), one gets

$$-1/(L - z_i - s)(k\partial T/\partial \phi)_s + (k\partial T/\partial r)_s \sin\beta\cos\beta = q_{i,n}\sin\beta = [q_{0,n} - F\rho(\partial s/\partial t)\sin\beta]\sin\beta \quad (7)$$

Thus, the temperature gradient, $(\partial T/\partial \phi)_s$, at the surface in the transformed coordinates is related to the normal component of the external heat flux $q_{0,n}$, the instantaneous recession rate, $(\partial s/\partial t)\sin\beta$, and (when β is not 90°) the tangential temperature gradient at the surface, $(\partial T/\partial r)_s$, resulting from cumulative transverse thermal conduction from the initial instant. For materials like beryllium which have a well-defined melting point, the surface temperature remains constant when melting occurs. Under such conditions, the recession rate is calculated by evaluating Eq. (4) at the surface and setting $\partial T/\partial t$, equal to zero; in other words, the liquid layer is assumed to be negligibly thin.

For convenience, it is assumed that the back face is insulated so that,

$$(\partial T/\partial \phi)(r,l,t) = 0$$

In addition, the axial symmetry requires:

$$(\partial T/\partial r)(0,\phi,t) = 0 \quad (8)$$

d) *Local heat-transfer rates and freestream conditions*

Since the time-dependent ablation rate is different along the ablating surface, the body shape changes accordingly. This leads to changes in flow around the body and consequently in local heat-transfer rates. These effects have been taken into account by properly evaluating the instantaneous boundary-layer growth by the use of the Howarth-Dorodnitsyn transformation,[4] in other words, so that $q_0 t$ is zero in this study $q_{0,n}$ is calculated from the following expression for a laminar-

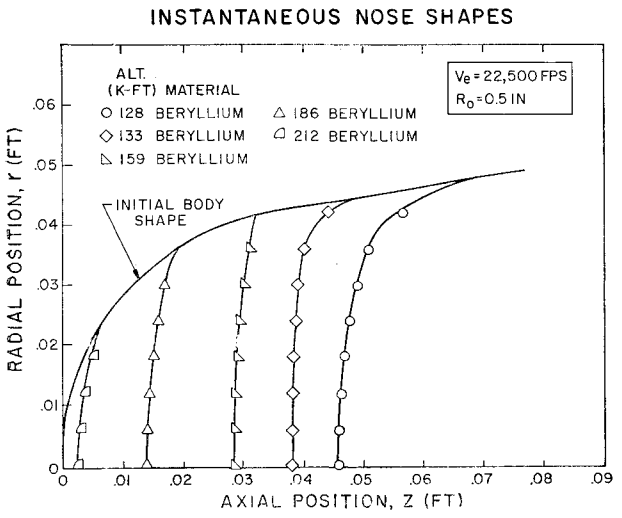

Fig. 2 Instantaneous nose shapes and radii.

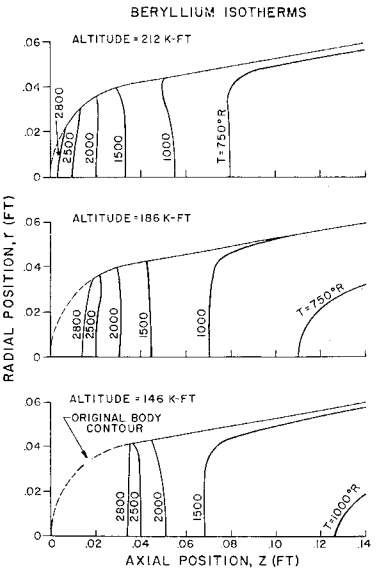

Fig. 3 Instantaneous internal temperature distribution.

boundary layer:

$$q_{0,n} = 0.45(k\rho/c_p)_w[u_e r/(2\xi)^{1/2}](H_e - H_w) \tag{9}$$

where

$$\xi = \int_0^x \rho_e \mu_e u_e r^2 dx \tag{10}$$

$$H_e = c_p T_\infty + u_\infty^2/2 \tag{11}$$

and

$$H_w = c_p T_w$$

As the surface changes in shape, the inviscid flow changes also. For simplicity, the freestream conditions outside the boundary layer are determined by assuming a Newtonian pressure distribution. This assumption reveals most of the basic phenomena. More accurate models for the surface pressure were not investigated in the present study. For the assumed pressure distribution,

$$(p_e - p_\infty)/(p_{st} - p_\infty) = \cos^2[(\pi/2) - \beta] \tag{12}$$

The inviscid flow along the surface is assumed to have a constant ratio of specific heats, thus

$$\rho_e/\rho_{st} = (p_e/p_{st})^{1/\gamma} \tag{13}$$

The velocity in the inviscid flowfield is obtained by isentropic expansion of the gas from the stagnation point, yielding

$$u_e^2/2 = H_e[1 - (p_e/p_{st})^{(\gamma-1)/\gamma}] \tag{14}$$

It is interesting to note that the heat-transfer rates computed from Eq. (9) are closely coupled to body shapes and weakly coupled to surface temperatures which are changing during transient heating. For problems where radiative heat loss is important (like graphite) $q_{0,n}$ as calculated from Eq. (9) should be reduced by an amount due to radiation before it is substituted into Eq. (7) for evaluating the boundary condition. The conditions at the stagnation point (p_{st}, ρ_{st}, etc.) are obtained from normal-shock relationships for equilibrium air.[5]

At the stagnation point, Eq. (9) leads to the following limiting expression:

$$(q_{0,n})_{st} = 0.45\left(\frac{k}{c_p}\right)_w\left(\frac{2}{\rho_e\mu_e}\right)_{st}^{1/2}\left(\frac{du_e}{dx}\right)_{st}^{1/2}(H_e - H_w) \tag{15}$$

where

$$(du_e/dx)_{st} = (1/R_n)(2p_{st}/\rho_{st})^{1/2} \tag{16}$$

and, for an axisymmetric body

$$R_n = (-r_{st}''')^{-1/2} \tag{17}$$

The conditions at the edge of the boundary layer were taken initially as Newtonian, see Eq. (12), except when the nose blunted to a degree where it is no longer valid; in such cases, the heating was assumed to be that for a flat-faced body.

Near the stagnation point, where ξ is extremely small, $q_{0,n}$ computed from Eq. (9) may be greatly in error. Thus, the following expansion (valid to the order of x^2) is used instead

$$(q_{0,n})/(q_{0,n})_{st} = 1 - Ex^2 \tag{18}$$

$$E = \{r'''_{st}\left\{\frac{5}{36} - \frac{1}{3\gamma}\left[\frac{3}{2} + \omega(\gamma - 1)\right]\right\} + \frac{r_{st}{}^{v}}{36 r_{st}'''} \tag{19}$$

We have taken $r_{st}{}^{iv} = 0$, which is correct for both a sphere and a paraboloid. Because of the difficulty of calculating $r_{st}{}^{v}$ numerically, it was assumed to have the value corresponding to a sphere of radius

$$(-r_{st}''')^{-1/2}$$

see Eq. (17). This approximation should cause very little loss in generality of the results obtained. ω is the temperature exponent for viscosity variation, such that

$$\mu_e/\mu_{st} = (T_e/T_{st})^{\omega} \tag{20}$$

e) Numerical technique

The coupled equations presented in the previous sections have been solved numerically by an explicit technique with the aid of an IBM 360/44 computer. Because of the strong coupling between the instantaneous body shape and heat-transfer rate, the numerical scheme tends to be unstable when the nose radius changes abruptly. To assure a gradual temporal variation of the nose radius, it has been found useful to employ a Taylor-series expansion in terms of Δt (time increment of marching procedure), such that

$$(R_n)_{t+\Delta t} = (R_n)_t\{1 - [R_n(\partial^2/\partial r^2)(\partial s/\partial t)]_t \Delta t\} \tag{21}$$

The spatial grid size (Δ_r, Δz) and time Δt are chosen such that

$$(\alpha \Delta t/\Delta r(\Delta z)_{\min}) < 0.02 \tag{22}$$

The numerical technique seems to be stable when the above criterion is satisfied.

III. Results

Calculations were performed for a typical re-entry vehicle of sphere-cone configuration. Since the main interest was to

examine the nose tip region, the results presented here cover only a small portion of the total length of the vehicle in the axial direction. The physical dimensions of the nose tip as indicated by the sketch in Fig. 1 are the following: initial nose radius (R_n) of 0.5 in., axial length (L), 3.6 in., cone half-angle (δ), 10°, radial coordinate of the cut-off point (R), 0.72 in. It is assumed that this portion of the vehicle is homogeneous and calculations were carried out for beryllium. The trajectory was assumed to be typical for a re-entry vehicle; namely, re-entry velocity of 22,500 fps, re-entry angle of 20°, ballistic parameter of 1000 lb/ft.[2] It should be pointed out that for the altitude range for which data are presented vehicle slowdown is unimportant. The vehicle is assumed to re-enter the atmosphere at 300 Kft altitude with a uniform initial temperature of 540°R.

For purposes of this calculation it was assumed that the liquid beryllium is immediately removed from the surface after melting and neither the liquid nor the vapor (if vaporized) absorbs any additional heat from the external flowfield.

Fig. 2 shows the ablated shapes at various altitudes. The increase in nose radius is of over 30 times its initial value at 140 Kft. It is also interesting to note the alternate blunting and sharpening of the nose with altitude as the different parts of the body begin to reach melting temperature. It is thus expected that for materials like beryllium, the three-dimensional effects due to coupling between instantaneous heat-transfer rate and body shape become very important.

Fig. 3 shows the isotherms in the nose region at various altitudes. By visualizing lines normal to these isotherms as representing heat-flow direction, one may conclude that thermal conduction is mainly normal to the surface near either the stagnation region or the downstream conical portion of the nose. However, in the intermediate region near the initial sphere-cone junction, heat conduction parallel to the surface becomes important.

IV. Conclusions

The results of this study show that both body-shape change and three-dimensional heat conduction should be considered in the treatment of an ablating, blunt-shaped object. They are necessary for two reasons: a) to account for both radial and axial thermal conduction in the solid, and b) to couple instantaneous body shape with the shape-dependent external heating environment.

Beryllium exhibits major changes in the instantaneous body shape. Severe nose blunting causes a large decrease in the aerodynamic heating rate over the blunted region, thus significantly reducing its recession rate. The portion of the body where the blunted region joins the unmelted part, however, experiences large increases in the heating rate, leading thus to ablation of these corners soon afterwards. The result is a nose-sharpening period during which the radius of curvature decreases and the heating rate in the blunted region increases. These blunting and deblunting periods alternate as different parts of the vehicle undergoes melting. For further details, and an idealized calculation of graphite ablation with axisymmetric heat conduction, the reader is referred to Ref. 6.

References

[1] Benjamin, A. S., "The Effect of Ablative Geometry Change on the Heating and Recession Characteristics of Sphere-Cones," AIAA Paper No. 66-992, Boston, Mass.

[2] Karachima, K., Kubota, H., and Sato, K., "An Aerodynamic Study of Ablation Near the Region of Stagnation Point of Axially Symmetric Bodies at Hypersonic Speeds," Rept 425, 1968, Institute of Space and Aeronautical Science, University of Tokyo, Tokyo, Japan.

[3] Landau, H. G., "Heat Conduction in a Melting Solid," *Quarterly of Applied Mathematics*, Vol. 8, No. 81, 1950.

[4] Lees, L., "Laminar Heat Transfer Over Blunt Nosed Bodies at Hypersonic Flight Speeds," *Jet Propulsion*, Vol. 26, April 1956, pp 259–269.

[5] Feldman, S., "Hypersonic Gas Dynamic Charts for Equilibrium Air," Avco Research Rept. 40, Jan. 1957.

[6] Popper, L. A., Toong, T. Y., and Sutton, G. W., "Axisymmetric Ablation with Shape Changes and Internal Heat Conduction," AIAA Paper No. 70-199, New York, 1970.

Laser Schlieren Crossed-Beam Measurements in a Supersonic Jet Shear Layer

B. H. Funk* and K. D. Johnston*

NASA Marshall Space Flight Center, Huntsville, Ala.

Nomenclature

e	=	deviation from time-averaged signal voltage
N_o	=	ambient index of refraction
S	=	schlieren sensitivity
t	=	time
U	=	flow speed
x,y,z	=	nozzle-fixed coordinates (Fig. 1)
α	=	Gladstone-Dale constant
ξ,η,ζ	=	beam-fixed coordinates (Fig. 1)
ρ	=	density
ρ'	=	deviation from time-averaged density
τ	=	time lag
τ_P	=	time lag at which maximum correlation occurs

Subscripts

c	=	convection
e	=	nozzle exit
H	=	horizontal beam
V	=	vertical beam

Introduction

THE optical crossed-beam technique has heretofore been used to measure statistical properties of turbulent flow by monitoring the fluctuations in light intensity caused by random fluctuations of the absorption or scattering coefficients.[1,2] Local information is retrieved by cross correlating the random outputs of two photodetectors that measure the fluctuating intensity of two mutually perpendicular light beams.

In addition to absorption and scattering, index of refraction fluctuations can also produce signal fluctuations; however, in the previous ultraviolet absorption crossed-beam experiments, this effect was minimized by the optical design. The potency of the schlieren effect for crossed-beam measurements

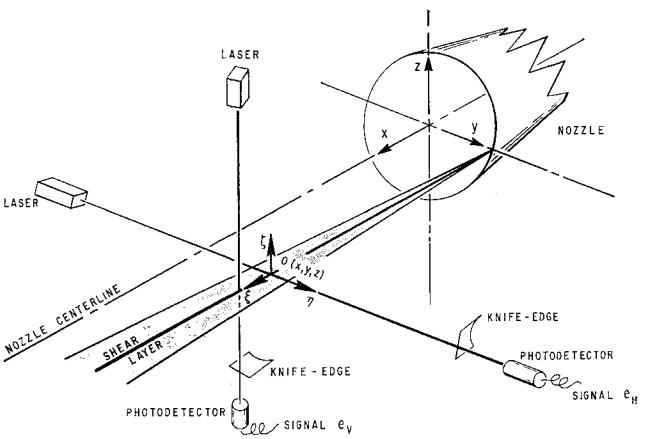

Fig. 1 Laser schlieren crossed-beam arrangement.

Received July 16, 1970.

* Aerospace Engineers.